In CT the goal is to reconstruct the x-ray attenuation coefficient f inside the object being scanned. Local tomography (LT) computes not f, but $\mathcal{B}f$, where $\mathcal{B}$ is some operator that enhances singularities of f. In 2D, $\mathcal{B}$ is an elliptic PDO of order one.

See papers by A. Faridani, D. Finch, A.K., P. Kuchment, F. Natterer, T. Quinto, A. Ramm, E. Ritman, K. Smith, and others on various aspects of LT.

Example of 2D local tomography

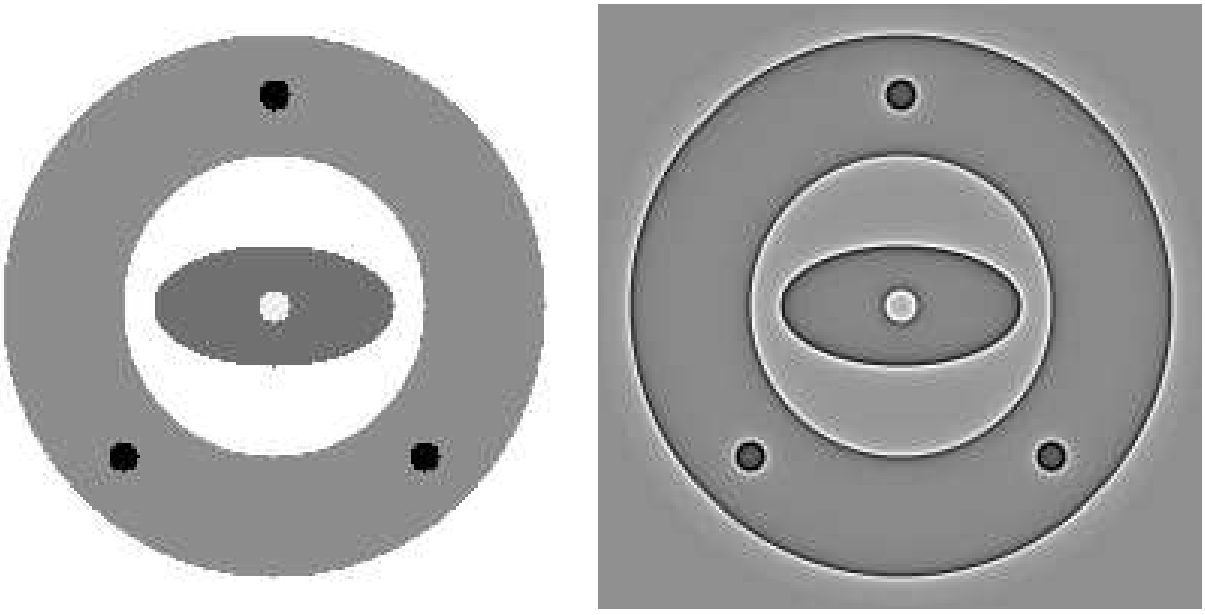

Left panel - original phantom f, right panel - local tomography function $\mathcal{B}f$.

Cone beam CT

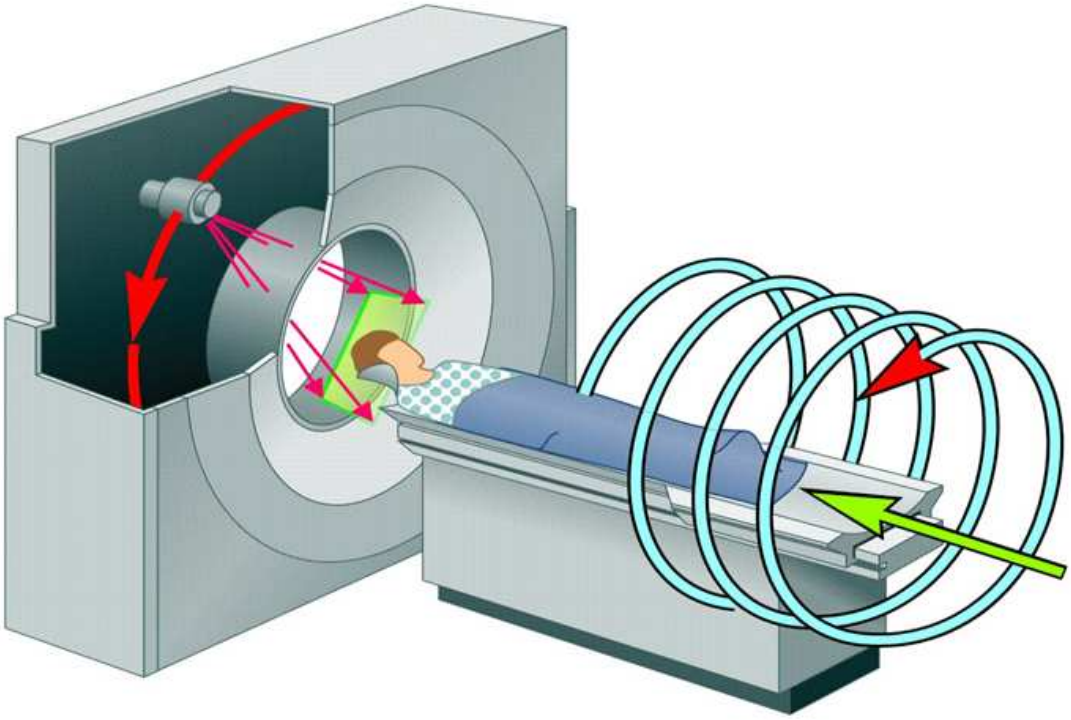

In the cone beam setting (3D) a LT function, which we denote here g_{Λ}, was introduced by A. Louis and P. Maass in 1993, and further studied by A.K. in 1999 and D. Finch and I.-R. Lan also in 1999.

It turned out that the corresponding operator $\mathcal{B}: f \to g_\Lambda$ is much more complicated than in 2D. It preserves visible (or, useful) singularities of f (this term was introduced and studied by T. Quinto in the setting of limited data inversion), but creates also non-local artifacts. Unfortunately, the strength of these artifacts is the same as that of the useful singularities of g_Λ.

Examples

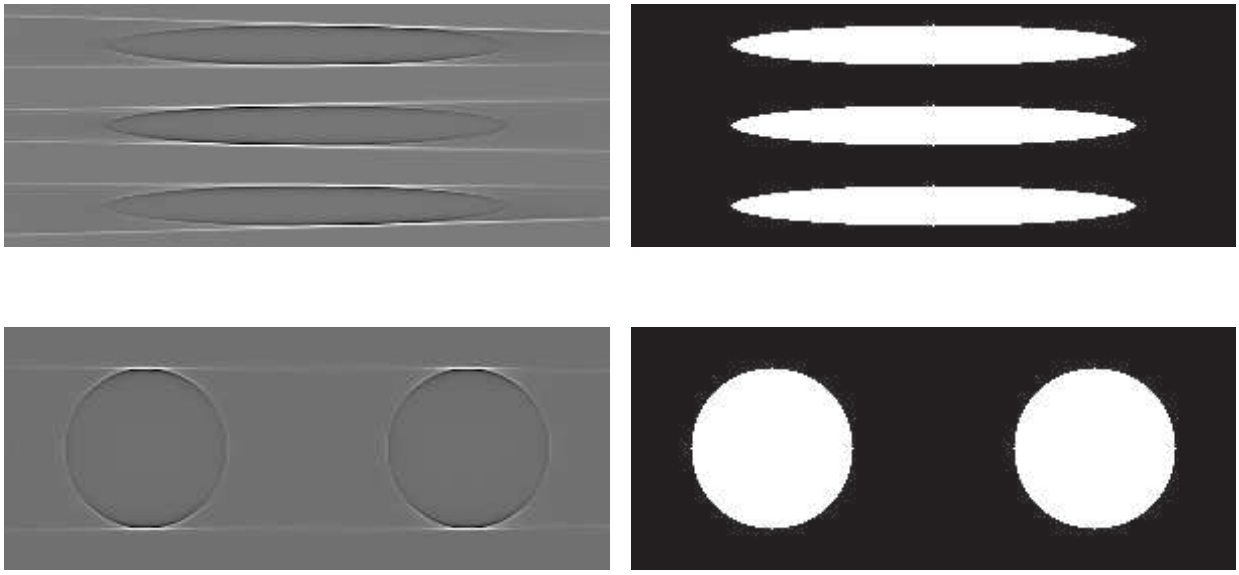

Left panel - g_Λ, right panel - original phantom.

Outline of the talk

In this talk we propose a new cone beam LT function g. We show that, similarly to g_Λ, g recovers the visible singularities of f. More precisely, the operator $f \to g$ is just a PDO of order one microlocally near the visible singularities of f.

The main advantage of the new LT function is that it produces artifacts, which are one order smoother in the scale of Sobolev spaces than the artifacts produced by g_Λ.

Remark: As follows from the works of A. Greenleaf and G. Uhlmann, see also a nice recent review paper by D. Finch, I.-R. Lan, and G. Uhlmann, non-local artifacts are inherent in cone beam LT.

Next we investigate how LT works when f changes with time. One of the applications - cardiac imaging.

We assume that f is a conormal distribution, which depends smoothly on time. The notion of visible singularities is suitably generalized, and a relationship between $WF(f)$ and $WF(g)$ is established. Interestingly, even the visible singularities of f no longer coincide with the corresponding singularities of g. There is a shift between them, and its size depends on the rate of change of f. We also investigate non-local artifacts in g, and they turn out to be of the same strength as in the static case (i.e., weaker than in g_Λ).

Finally, we discuss some implementation issues when the source trajectory is a helix and present numerical experiments both in the static and dynamic cases.

New LT function

Let C be a smooth curve:

$$I \ni s \to y(s) \subset \mathbb{R}^3,$$

$D_f(s,\alpha)$ denote the cone beam transform of f:

$$D_f(s,\alpha) = \int_0^\infty f(y(s)+\alpha t)dt,\ \ s \in I,\, \alpha \in S^2,$$

where $f \in C_0^\infty(V)$ and V is an open set with $\overline{V} \subset \mathbb{R}^3 \setminus C$.

Fix $\varphi \in C_0^\infty(I \times V)$ and define:

$$\begin{aligned} g(x) &:= (\mathcal{B}f)(x) \\ &:= \int_I \varphi(s,x)\, \frac{\partial^2}{\partial q^2} D_f(s,\beta(q,x))\Big|_{q=s} ds, \end{aligned}$$

where

$$\beta(q,x) := \frac{x-y(q)}{|x-y(q)|}.$$

Comparison of new and old LT functions

New function:

$$g(x) := \int_I \varphi(s,x)\, \frac{\partial^2}{\partial q^2} D_f(s,\beta(q,x))\Big|_{q=s} ds.$$

Here

$$\frac{\partial^2}{\partial q^2} D_f(s,\beta(q,x))\Big|_{q=s}$$

is the second derivative on the detector along the "projection of the source trajectory".

Old function (one of the versions):

$$g_\Lambda(x) := \int_I \varphi(s,x) \Delta_x D_f(s,\beta(s,x)) ds.$$

Here

$$\Delta_x D_f(s,\beta(s,x))$$

is the Laplacian on the detector (loosely speaking).

Additional notation

$$\Pi(x,\xi) := \{y \in \mathbb{R}^3 : \ \xi \cdot (y-x) = 0\},$$

$$WF_v(f) := \{(x,\xi) \in WF(f) : \ \Pi(x,\xi) \text{ intersects } C \text{ transversely}\},$$

$$L_+(s,z) := \{x \in \mathbb{R}^3 : \ x = y(s) + t(z - y(s)), \ t > 0\}.$$

Proposition. The operator $f \to g$ extends to a map $\mathcal{E}'(V) \to \mathcal{E}'(V)$, and

$$WF(g) \subset WF_v(f) \cup E(f, C).$$

Here $WF_v(f)$ are the visible singularities of f, and $E(f, C)$ is the non-local artifact.

Illustration of the artifact

An equivalent definition of the set $E(f, C)$ is as follows. If $(z, \xi) \in WF(f)$ and the plane $\Pi(z, \xi)$ is tangent to C at some point $y(s)$, then $(x, \xi) \in E(f, C)$ for all $x \in L_+(s, z)$, $(s, x) \in \operatorname{supp} \varphi$.

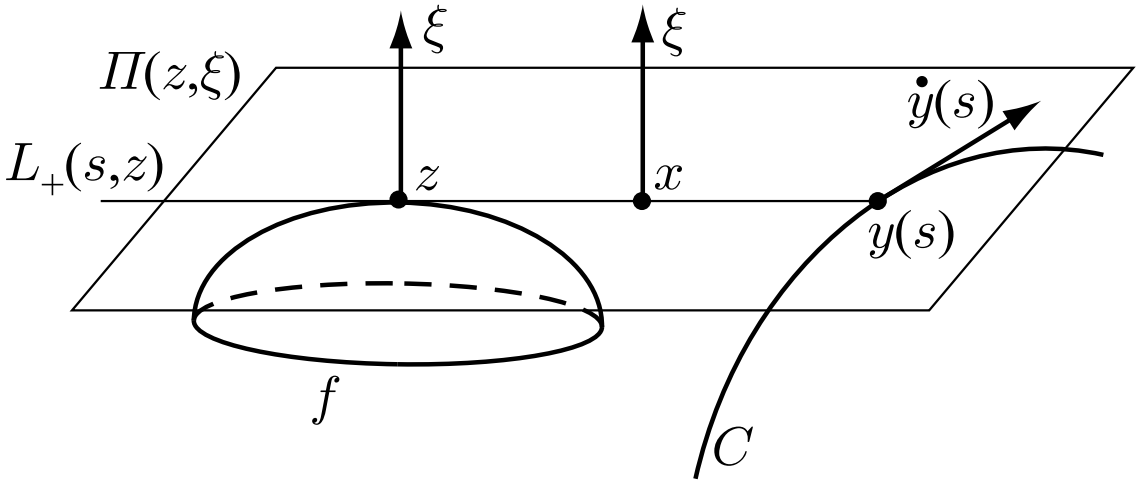

The principal symbol of $\mathcal{B}$

One has

$$(\mathcal{B}f)(x) = \frac{1}{(2\pi)^3} \int_{\mathbb{R}^3} \tilde{f}(\xi) B(x,\xi) e^{-i\xi\cdot x} d\xi.$$

Pick $(x,\xi) \in T^*V \setminus 0$ such that $\Pi(x,\xi)$ intersects C, and the intersections are transversal. Then

$$\begin{aligned} B(x,\sigma\xi) = &- 2\pi\sigma \sum_j \varphi(s_j,x)|x - y(s_j)||\xi \cdot \dot{y}(s_j)| \\ &+ O(1), \quad \sigma \to \infty. \end{aligned}$$

Thus $\mathcal{B}$ has the principal symbol of order one microlocally near visible singularities (similarly to the old LT operator).

Analysis of artifacts

Pick any $(z_0, \xi_0) \in WF(f)$ s.t. $\Pi(z_0, \xi_0)$ is tangent to C at some $y(s_0)$. What is the behavior of g in a neighborhood of $x_0 \in L_+(s_0, z_0)$?

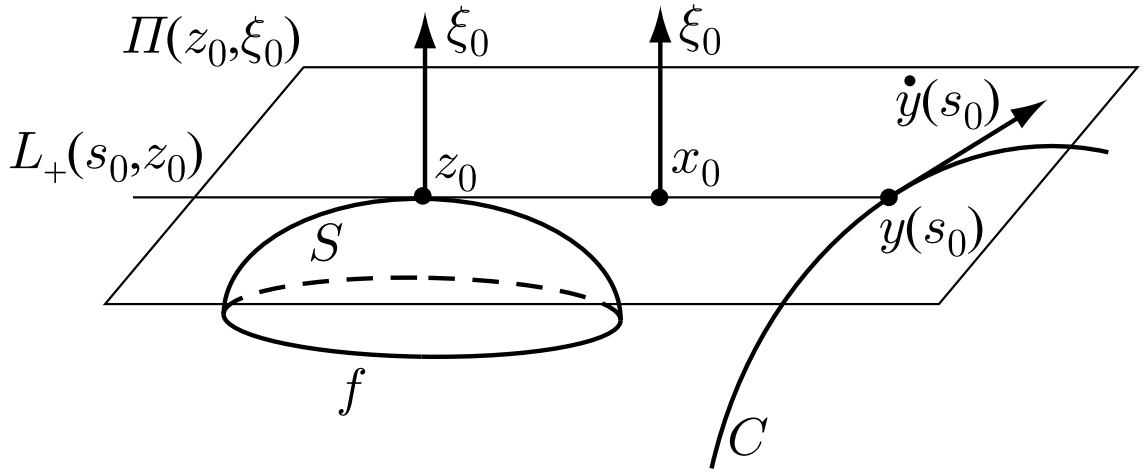

Assume that f is a conormal distribution associated to a smooth hypersurface S with nonzero Gaussian curvature at z_0.

$\tilde{f}(\xi) = A(\xi)e^{iH(\xi)}$ m./loc. near (z_0, ξ_0), where $A(\xi) \in S^m(\mathbb{R}^3)$ and $N^*S = (H'(\xi), \xi)$.

Strength of artifacts

New function

$$g(b,\rho) \sim c_1 \left(\frac{c}{b-c}\rho + i0\right)^{-(m+2)}, \ \rho \to 0.$$

Old function

$$g_\Lambda(b,\rho) \sim c_2 \left(\frac{c}{b-c}\rho + i0\right)^{-(m+3)}, \ \rho \to 0.$$

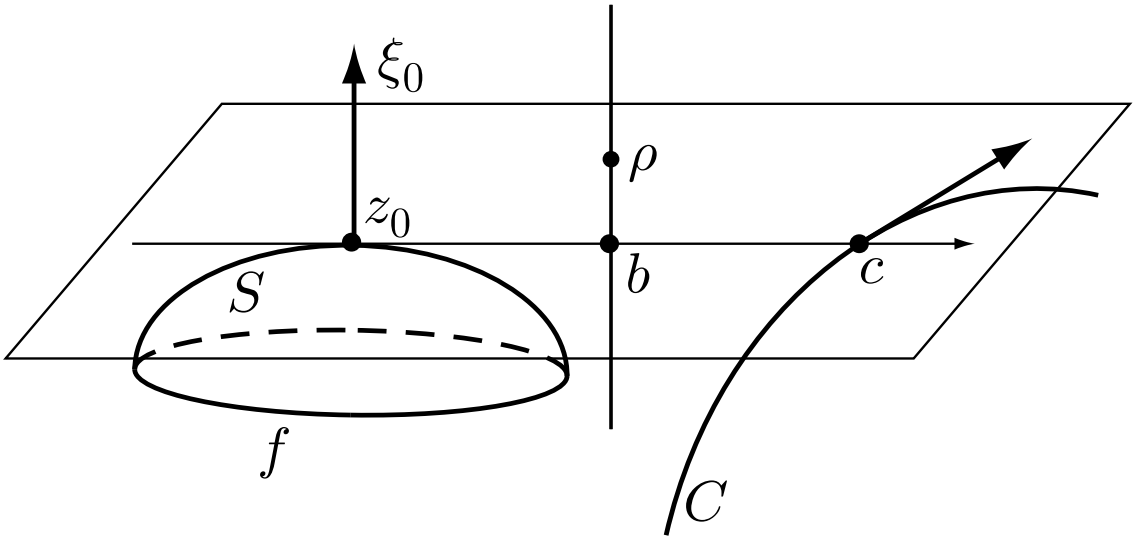

Dynamic local tomography

Now f changes with time. Since usually the parameter s in the definition of the curve C can be regarded as time, we can assume that f is of the form $f(s,x)$, and the cone beam data are

$$D_f(s,\alpha) = \int_0^\infty f(s, y(s) + \alpha t)dt, \ \ s \in I, \, \alpha \in S^2.$$

The LT function is still defined by the same formula:

$$g(x) := \int_I \varphi(s,x) \, \frac{\partial^2}{\partial q^2} D_f(s, \beta(q,x))\Big|_{q=s} ds.$$

Proposition. The operator $\mathcal{B}$ extends to a map $\mathcal{E}'(I \times V) \to \mathcal{E}'(V)$.

Action on wave fronts

Consider the case when f is a conormal distribution, which depends smoothly on s. Pick an arbitrary

$$(s_0, z_0, \eta_0) \in I \times (T^*V \setminus 0).$$

Because of linearity, we can assume that:

1. supp f belongs to a small neighborhood of (s_0, z_0);
2. The Fourier transform of $f(s, z)$ with respect to z satisfies:

$$\tilde{f}(s, \eta) = A(s, \eta) e^{iH(s,\eta)}$$

microlocally near (z_0, η_0). Here $H''_{\eta\eta}(s_0, \eta_0)$ is non-degenerate and $A(s, \cdot) \in S^m(\mathbb{R}^3)$ uniformly in s.

Proposition. Let f be as above. $WF(g)$ is a subset of all $(x, \xi) \in T^*V \setminus 0$ which satisfy

$$y(s) + t(x - y(s)) = H'_\eta(s, \eta) \quad (1)$$
$$\eta \cdot \dot{y}(s)(1 - t) = H'_s(s, \eta) \quad (2)$$
$$\eta \cdot (x - y(s)) = 0 \quad (3)$$
$$\xi = t\eta \quad (4)$$

for some $(s, z = H'_\eta(s, \eta), \eta)$ close to (s_0, z_0, η_0).

(1) x, $y(s)$, and $z = H'_\eta(s, \eta)$ are on the same line;
(2) "Dynamic term". Determines the shift between x and z;
(3) x and $y(s)$ belong to the plane perpendicular to η;
(4) ξ and η are parallel.

Visible singularities.

Pick $(z, \eta) \in WF(f(s, \cdot))$ such that

$$y(s) \in \Pi(z, \eta) \cap C.$$

Suppose the intersection is transversal, that is $\eta \cdot \dot{y}(s) \neq 0$. The singularity (s, z, η) of f is called *visible*.

The corresponding singularity $(x, \xi) \in WF(g)$ is given by

$$x = z + (z - y(s))(t^{-1} - 1),$$
$$\xi = t\eta, \ t = 1 - \frac{H'_s(s, \eta)}{\eta \cdot \dot{y}(s)}.$$

Illustration.

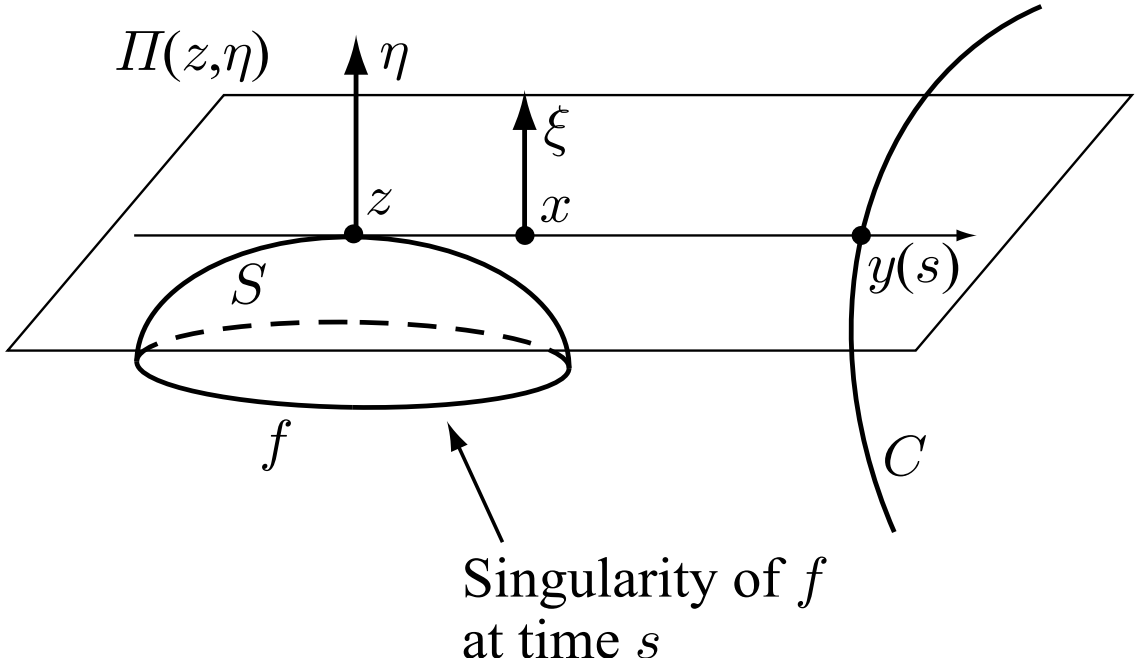

Artifacts.

Pick $(z, \eta) \in WF(f(s, \cdot))$ such that

$$y(s) \in \Pi(z, \eta) \cap C.$$

Suppose $\eta \cdot \dot{y}(s) = 0$ and $H'_s(s, \eta) = 0$.

The corresponding nonlocal singularity $(x, \xi) \in WF(g)$ is given by

$$x = y(s) + (z - y(s))/t,$$
$$\xi = t\eta, \ \forall t > 0.$$

Quantitative estimates.

Visible (or, useful) singularities.
Under our assumptions about f, the local tomography function $g = \mathcal{B}f$ is also a conormal distribution. A precise microlocal description of the corresponding Lagrangian manifold and the strength of g is obtained. It turns out that $\mathcal{B}$ enhances visible singularities in much the same way as in the static case.

Artifacts.
The artifacts here are of the same strength as in the static case.

Some details.

Proposition. Suppose $\Pi(z_0, \eta_0) \cap C = y(s_0)$ and $\eta_0 \cdot \dot{y}(s_0) \neq 0$, where $z_0 = H'_\eta(s_0, \eta_0)$. Find (x_0, ξ_0) by solving (1)–(4). Let Ω be a sufficiently small open cone containing ξ_0. Solving the system (1)–(4) for s, t, x, and η in terms of $\xi \in \Omega$ determines $C^\infty(\Omega)$ functions $s(\xi)$, $t(\xi)$, $x(\xi)$, and $\eta(\xi)$. s, t, x are homogeneous of order 0, and η is homogeneous of order 1.

Denote $G(\xi) := \xi \cdot x(\xi)$. By the proposition, we can define a Lagrangian submanifold Λ of a conic neighborhood of (x_0, ξ_0):

$$\Lambda = \{(G'(\xi), \xi) : \xi \in \Omega\}.$$

Proposition. Let f be as above. Suppose $\Pi(z_0, \eta_0) \cap C = y(s_0)$ and $\eta_0 \cdot \dot{y}(s_0) \neq 0$. Find (x_0, ξ_0) by solving (1)–(4). Then the LT function is a distribution $g \in I^{(m+3/4)+1}(V, \Lambda)$, and for $|\xi| > 1$:

$$e^{-iG(\xi)}\tilde{g}(\xi) + 2\pi \frac{\varphi(s,x)|x - y(s)|}{t} |\eta \cdot \dot{y}(s)| A(s,\eta) \in S^m(\mathbb{R}^3),$$

where s, t, x, and η are the functions of ξ obtained by solving the system (1)–(4). $A(s, \eta)$ is interpreted as 0 if no solution exists. $e^{-iG(\xi)}\tilde{g}(\xi)$ is polyhomogeneous if A is.

Numerical experiments: static cases.

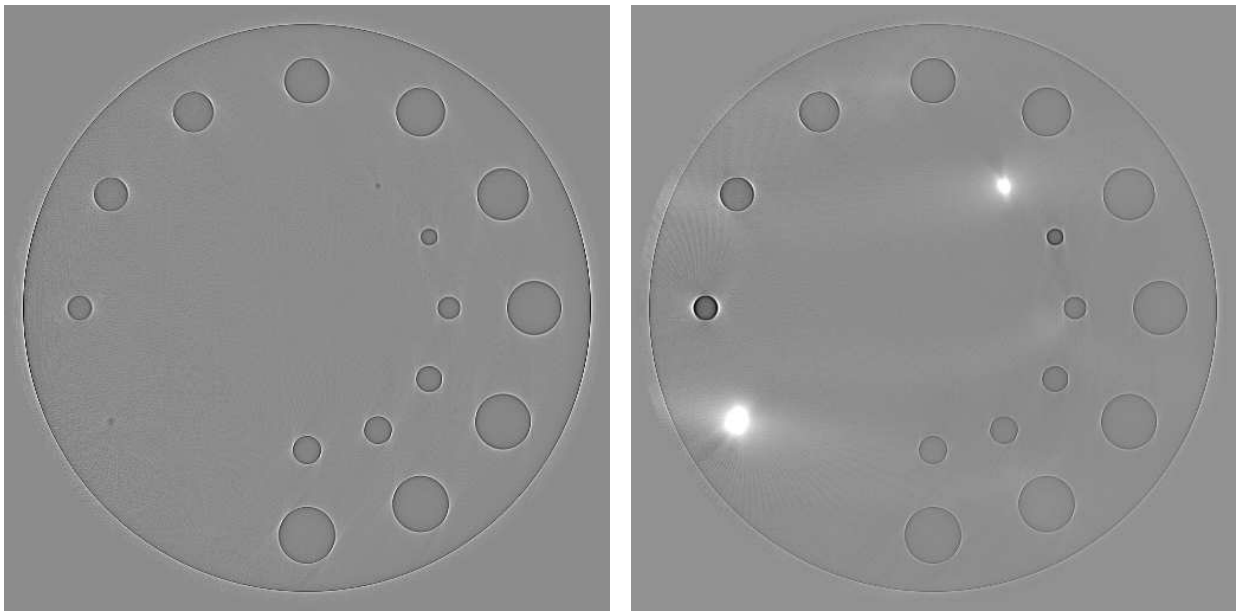

Reconstruction of the clock phantom. The cross-section $|x_1| \leq 255.5, |x_2| \leq 255.5, x_3 = 0$ is shown. Left panel - new LT function g, right panel - old LT function g_Λ.

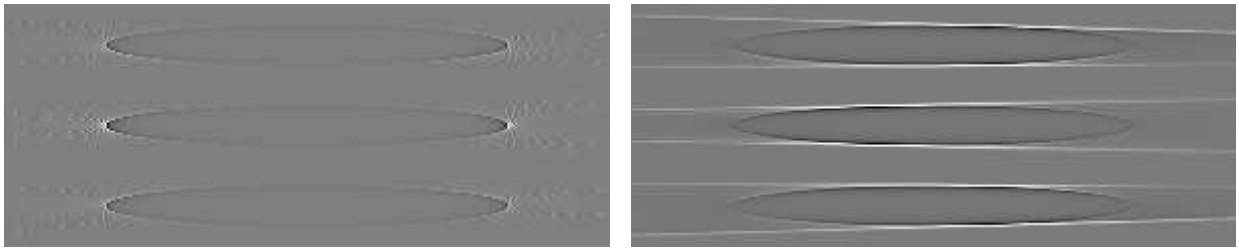

Reconstruction of the three-disk phantom. The cross-section $|x_1| \leq 150, x_2 = 0, |x_3| \leq 60$ is shown. Left panel - new LT function g, right panel - old LT function g_Λ.

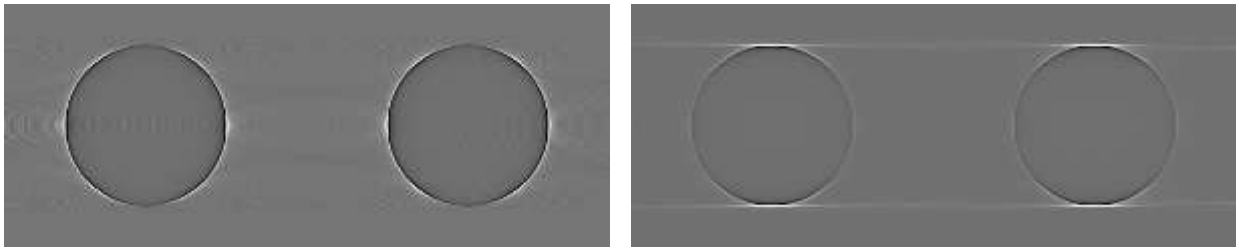

Reconstruction of the two-ball phantom. The cross-section $|x_1| \leq 150, x_2 = 0, |x_3| \leq 60$ is shown. Left panel - new LT function g, right panel - old LT function g_Λ.

Numerical experiments: dynamic cases.

Now the phantom is represented by a single ellipsoid

$$\left(\frac{x_1 - x_1(s)}{a(s)}\right)^2 + \left(\frac{x_2 - x_2(s)}{b(s)}\right)^2 + \left(\frac{x_3 - x_3(s)}{c(s)}\right)^2 \leq 1,$$

whose parameters – the half-axes $a(s)$, $b(s)$, $c(s)$, and the center $(x_1(s), x_2(s), x_3(s))$ – depend on time.

New LT function g.

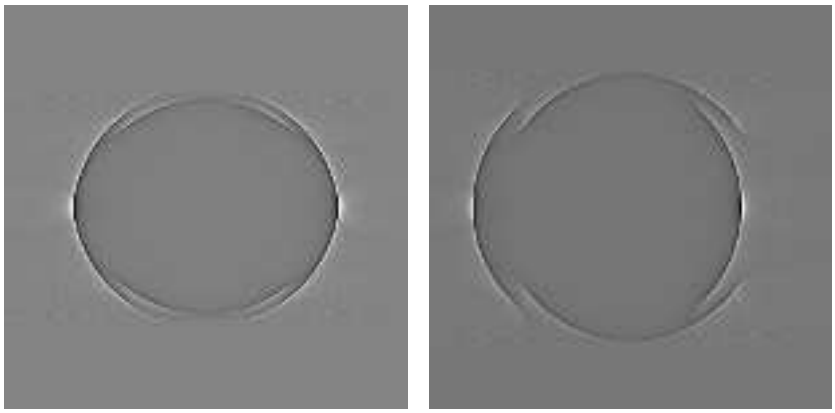

The ellipsoid moves either up-down (left panel) or left-right (right panel). The cross-sections $|x_1| \leq 75, x_2 = 0, |x_3| \leq 75$ are shown in both panels.

New LT function g.

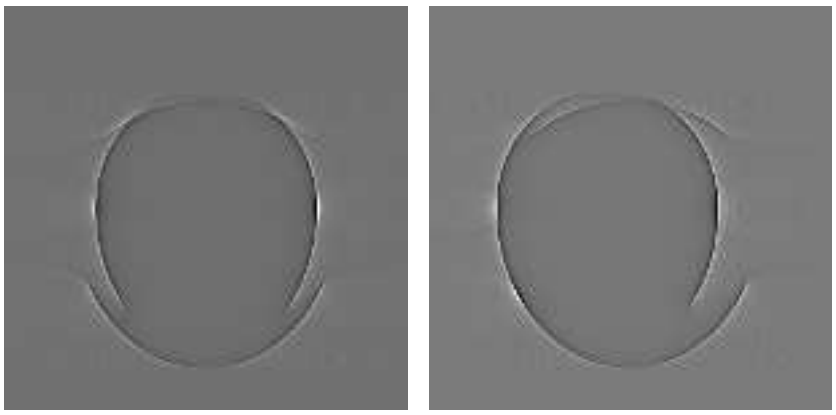

The ellipsoid either only expands and contracts (left panel) or expands and contracts as well as moves left-right (right panel). The cross-sections $|x_1| \leq 75, x_2 = 0, |x_3| \leq 75$ are shown in both panels.

New LT function g.

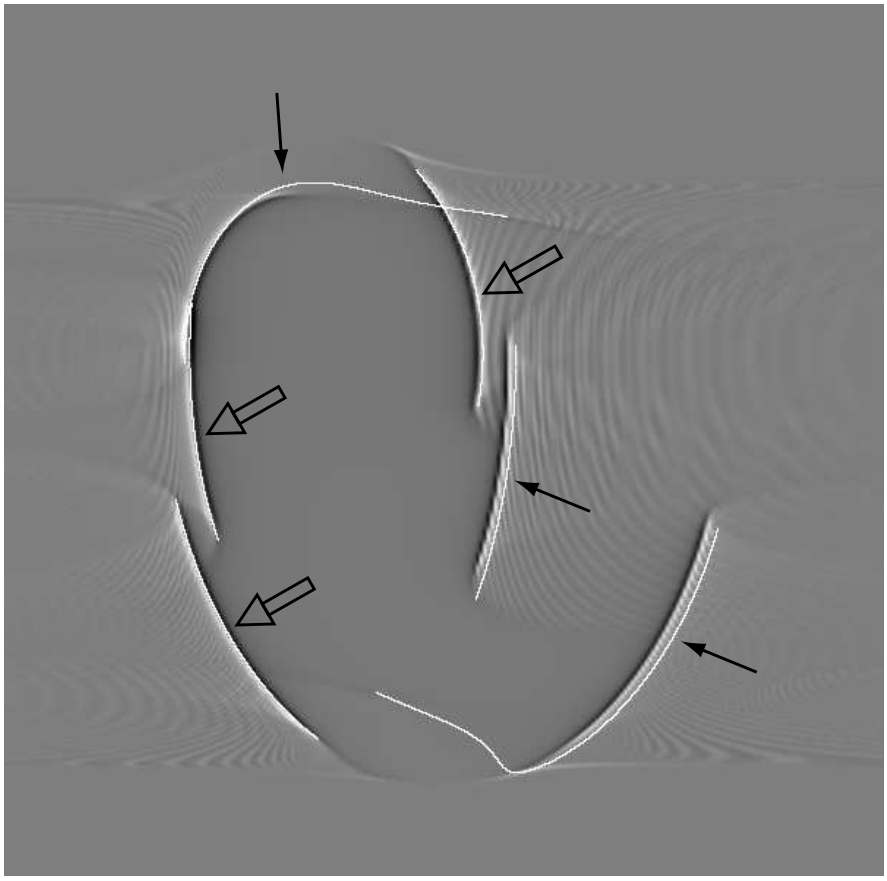

Illustration of the shift between the singularities of f and g in the dynamic case. The ellipsoid expands and contracts as well as moves left-right. The cross-section $|x_1| \leq 75, x_2 = 0, -90 \leq x_3 \leq 60$ is shown.

Conclusions

The preceding images have been obtained by ignoring the dynamic nature of the phantom. It is theoretically impossible to stably reconstruct an accurate 4D image of f (3D+time) from the cone beam data with only three degrees of freedom.

In many cases one can use additional information to improve image quality. Consider, for example, cardiac imaging based on a circular source trajectory. Using the ECG of the patient, which is measured concurrently with cone beam projections, one can accumulate projection data corresponding to a fixed cardiac phase (e.g., when the heart is at rest) from multiple source rotations and then perform LT reconstruction from only that data. Such techniques have been in use in conjunction with conventional inversion algorithms for a long time.

One can even solve approximately the problem of 4D CT imaging. Using again the ECG data, one splits the complete cardiac cycle into several segments, accumulates the cone beam data for each segment from multiple source rotations, and then applies LT separately for each segment.

Other ways of using LT for performing dynamic reconstructions might be possible.

Because of the significantly reduced x-ray dose to the patient, flexibility of LT, its relative stability with respect to inconsistencies in the data (compared with "global" algorithms) and the ability to accurately reconstruct edges inside objects, LT can become a valuable tool, which provides important information complementing well-established inversion techniques.